Journal of Molecular Structure 1287 (2023) 135724

Contents lists available at ScienceDirect

Journal of Molecular Structure

journal homepage: www.elsevier.com/locate/molstr

Synthesis, characterization, Suzuki-Miyaura and Mizoroki-Heck cross-coupling reactions of Schiff base-Pd(II) complexes

Abbas Akdeniz, Nevin Turan *

Department of Chemistry, Faculty of Arts and Sciences, Muş Alparslan University, Muş, Turkey

ARTICLE INFO

Keywords:
Pd(II) complex
Catalysis
Suzuki-Miyaura coupling
Mizoroki heck coupling
Characterization

ABSTRACT

Cross-coupling reactions are powerful and versatile tools mainly for the formation of carbon-carbon bonds in modern organic synthesis. The cross-coupling reactions catalyzed by palladium complexes have attracted a great deal of attention of researchers in recent years. Two new mononuclear Schiff base-Pd(II) complexes (1, 2) were synthesized and characterized by FT-IR, UV–Vis, NMR (^{1}H and ^{13}C), ESI-MS, CHNS analysis, magnetic susceptibility, molar conductivity, melting points, thermogravimetric analysis in addition to powder X-ray diffraction and SEM-EDX analysis. Depending on spectral and magnetic measurements, the suggested geometrical shapes of these complexes were reported. Further, Suzuki-Miyaura and Mizoroki-Heck cross-coupling reactions, using K_2CO_3 as base and Et-OH+H_2O (1:2) ration as solvent under atmospheric conditions, were carried out with the synthesized complexes in the presence of various aryl halides, phenylboronic acid, and styrene. Schiff base-Pd(II) complexes (1, 2) were found to provide very good yields in Suzuki-Miyaura and Mizoroki-Heck cross-coupling reactions. The results showed that electron-donating and electron-withdrawing substituents on the aryl halides might produce coupling products in perfect yield in the presence of Pd(II) complexes 1 and 2.

1. Introduction

Schiff bases are the most studied ligand class due to their high solubility, chelating ability, and stability. They have wide applications in transition metal chemistry. Schiff bases have electron rich donor atoms (N, O, and/or S) so they draw more attention in synthesis chemistry [1,2]. Since they can catalyze the oxidation of organic molecules and polymers, they are used in the industry [3,4]. They have a wide application area as coordination chemistry, biological activities, medicine, pharmacy, industry, magnetism, food packaging, paints, and polymer [5–7]. Schiff base complexes are used as the catalyst for polymerization, cross-coupling, and epoxidation reactions [8]. Cross-coupling reactions are the most effective reactions among these reactions. They are commonly used for syntheses of C—O, C—N, C—C, and C–S bonds [9]. The formation of C—C bands takes place through the Suzuki-Miyaura cross-coupling reaction. These are frequently used in medicine, material science, catalysis, and many fields [10]. Nickel and palladium are widely used as catalysts for coupling reactions. The most important reason for its catalytic activity is the flexibility in the exchange of its oxidation state, Pd(II)/Pd(0). Recently, Schiff base-Pd(II) complexes have attracted great attention in different fields from biological applications to catalysis [11–13]. These complexes are used as catalysts in Suzuki-Miyaura, Mizoroki-Heck reactions, allylic alkylation, etc. [14–17]. Pd(II) complexes containing N, O donor ligands show higher catalytic activity in the C—C coupling reaction than commercially used ligands containing phosphine metal complexes. Also, nitrogen-based ligands are popular in coordination chemistry as they can be easily modified both sterically and electronically [18].

As a part of our ongoing research on the synthesis and applications of transition metal complexes, herein, we have reported the synthesis and characterizations of two mononuclear Schiff base-Pd(II) complexes (1, 2) and the catalytic potential of palladium complex for Suzuki-Miyaura and Mizoroki Heck cross-coupling reactions. This article aims to reveal a new class of compounds that are easy and inexpensive to synthesize, and that Schiff base-Pd(II) complexes as high-efficiency catalysts may be promising candidates for catalysis.

2. Experimental

2.1. Physical measurements and reagents

Analytical-grade chemicals and solvents were provided by commercial suppliers (Merck and Sigma Aldrich). The elemental analyses were conducted by using the Leco CHNS-O model 932 elemental

* Corresponding author.
E-mail address: n.turan@alparslan.edu.tr (N. Turan).

https://doi.org/10.1016/j.molstruc.2023.135724
Received 21 February 2023; Received in revised form 19 April 2023; Accepted 4 May 2023
Available online 5 May 2023

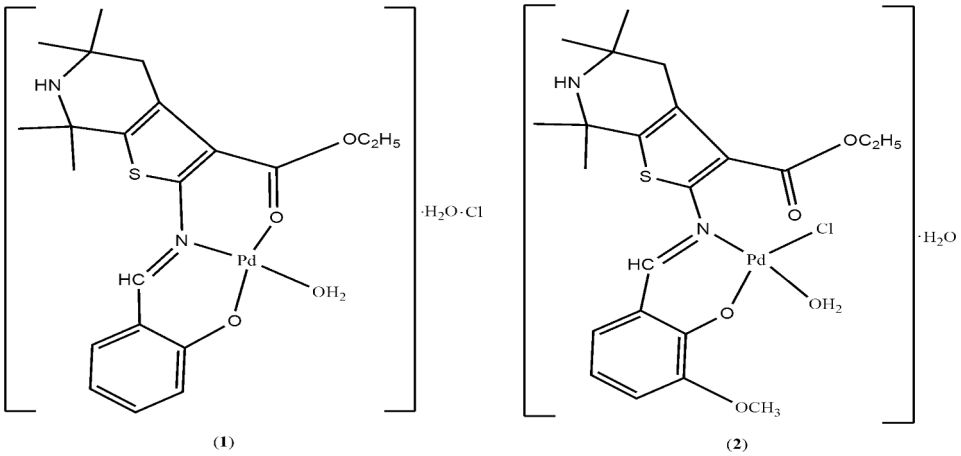

Fig. 1. The suggested structure of Schiff base-Pd(II) complexes.

analyzer. The Perkin Elmer Precisely Spectrum One FT-IR 65 spectrophotometer was used to measure IR spectra in the region of 4000–400 cm^{-1}. The ^{1}H and ^{13}C NMR spectra were performed on a Bruker GmbH DPX-400 MHz FT. The UV–vis. spectra were carried out on a Shimadzu 1800 spectrophotometer. Magnetic susceptibility was measured on a Sherwood Scientific Magnetic Susceptibility Balance MK1. Thermal analysis was done using a Shimadzu DTG-60 AH with 10 °C/min and nitrogen atmosphere. The mass spectra were carried out using an AGILENT model 1100 MSD mass spectrometer. Powder XRD analysis was performed using an UltimaIV X-ray diffractometer with Rigaku (CuKα=1.540562 A°). GCMS– were recorded on a GC–MS AGILENT model 7890 GC, 5977 MSD spectroscopy. The conductivity of prepared complexes was recorded via the Jenway 4010 conductivity meter in DMSO. Thermo-9100 was used to determine the melting point. SEM-EDX analyses were performed using a Philips XL30 SFEG scanning electron microscope (SEM) coupled to an energy dispersive spectrometer by EDAX (EDS). SEM was operated at 15 kV accelerating voltage.

2.2. Synthesis and characterization of the Schiff base-Pd(II) complexes

A toluene solution (15 mL) of $PdCl_2(CH_3CN)_2$ 0.36 g (1.4 mmol) was put in to the toluene solution (20 mL) of the Schiff base ligand, (*E*)-ethyl 2-(2-hydroxybenzylideneamino)−5,5,7,7-tetra methyl-4,5,6,7-tetrahydrothieno[2,3-*c*]pyridine-3-carboxylate (L^1), 0.40 g (1.4 mmol). This mixture was refluxed for 6 h at 90 °C. The light brown product was washed with diethyl ether and toluene. The precipitate was recrystallized from dichloromethane/diethyl ether. A similar method was followed to synthesize complex 2. (*E*)-ethyl 2-(2-hydroxy-3-methoxybenzylideneamino)−5,5,7,7-tetramethyl-4,5,6,7-tetrahydrothieno[2,3-*c*]pyridine-3-carboxylate (L^2) was used to obtain complex 2. The representation for the proposed structure were given in Fig. 1. The spectral and physical data are as follows:

[L^1Pd(H_2O)]Cl·H_2O (1): Colour: Light brown; Yield: 78%; Melting point.: 227 °C; CHNS: Calc. for $C_{21}H_{29}N_2O_5SPdCl$: C, 44.77; H, 5.19; N, 4.97; S, 5.69%, Found: C, 44.70; H, 5.17; N, 4.98; S, 5.65%; FT-IR (KBr, ν cm^{-1}): 3435 (-OH)$_{br.}$, 3280 (-NH)$_{br.}$, 3056 (Ar. -CH), 2974, 2924 (Al. -CH), 1712 (C=O), 1596 (CH=N), 1543, 1521, 1458 (Ar. C=C), 1171 (C—O), 784 (C-S-C), 857 (H_2O), 575, 554 (Pd-O), 502, 460 (Pd-N); ^{1}HNMR (400 MHz, DMSO-d_6) δ, ppm: 10.27 (s, H, -NH), 8.87 (s, H, CH=N), 7.69–6.54 (m, *J*=7.19 Hz, 4H, Ar.-CH,), 4.31 (m, *J*=4.17 Hz, 2H, OCH_2–), 2.51 (s, 2H, pyridine), 1.31 (t, *J*=1.31 Hz, 3H, -OCH_2CH_3), 1.46–1.13 (s, 12H, -CH_3); ^{13}CNMR (100 MHz, DMSO-d_6) δ, ppm: 164.68 (C14), 160.46 (C25), 155.95 (C8), 149.51 (C23), 136.87, 136.02, 123.05, 120.11, 117.06 (C18–22), 133.29 (C6), 130.50, 115.82 (C9, C5), 60.78 (C28), 56.55, 56.05, 39.37 (C1, C3, C4), 40.62, 40.20 (C10, C11), 39.99, 39.37 (C12, C13), 14.33 (C29); UV–Vis. (λ_{max}, nm): 220, 230, 240, 305, 332, 357, 371, 395, 406, 418, 440, 495; Molar conductivity: 130 ohm^{-1} cm^2 mol^{-1}. MS [ESI]: *m/z* 562.390 (Calc.), 562.791 (Found) $[M\text{-}H]^+$.

[L^2PdCl(H_2O)]H_2O (2): Colour: Brick color; Yield: 76%; Melting point.: >250 °C; CHNS: Calc. for $C_{22}H_{31}N_2O_6SPdCl$: C, 44.53; H, 5.27; N, 4.72; S, 5.40%, Found: C, 44.60; H, 5.25; N, 4.74; S, 5.40%; IR (KBr, ν cm^{-1}): 3442 (OH/H_2O)$_{br.}$, 3206 (-NH), 3055 (Ar. -CH), 2977, 2933 (Al. -CH), 1709 (C=O), 1596 (CH=N), 1579, 1550, 1535 (Ar. C=C), 1168 (C—O), 863 (H_2O), 783 (C-S-C) 590, 550 (Pd-O), 499, 459 (Pd-N); ^{1}HNMR (DMSO-d_6) δ, ppm: 10.27 (s, H, -NH), 8.87 (s, H, CH=N), 7.49–6.67 (m, *J*=7.08 Hz, 3H, Ar. -CH), 4.32 (m, *J*=4.32 Hz, 2H, -OCH_2CH_3), 3.83 (s, 3H, OCH_3), 2.50 (s, 2H, -CH_2 pyridine), 1.34 (t, *J*=1.34 Hz, 3H, -OCH_2CH_3), 1.45–1.26 (s, 12H, -CH_3); ^{13}CNMR (DMSO-d_6) δ, ppm: 163.56 (C14), 160.47 (C17), 153.23 (C8), 150.66 (C23), 148.87, 137.75, 124.62, 119.67, 117.41 (C18–22), 135.75 (C6), 1329.49, 117.88 (C9, C5), 61.61 (C28), 59.61, 56.37, 56.24, 38.49 (C1, C3, C6, C4), 40.49, 40.08 (C10, C11), 39.82, 39.49 (C12, C13), 14.54 (C29); UV–Vis (λ_{max}, nm): 217, 225, 243, 261, 304, 314, 324, 334, 349, 358, 363, 437, 495, 577; Molar conductivity: 15.60 ohm^{-1} cm^2 mol^{-1}. MS [ESI]: *m/z* 595.426 (Calc.), 595.906 (Found) $[M+2H]^{2+}$.

3. Results and discussion

3.1. Identification

The ligands L^1 and L^2 synthesized in the previous article were used in this study [19,20]. The spectroscopic data of the Pd(II) complexes (1, 2) were present in the experimental section. Elemental analysis (C, H, N, S) and mass spectra of the complexes are compatible with the suggested molecular structure. The palladium ions were coordinated to the ligands L^1 and L^2 in the ratio of 1:1. Complex 2 showed non-electronic behavior while complex 1 showed electronic behavior that has 130 ohm^{-1} cm^2 mol^{-1} value of molar conductivity and it confirmed that complex 1 was electrolyte.

The magnetic susceptibility of the Pd(II) complexes (1, 2) showed diamagnetic properties. The zero value of magnetic moment for the Pd (II) complex is characteristic of palladium in the tetra coordinated square-planar. In the ESI-MS of complexes 1 and 2, the peaks attributed to $[M\text{-}H]^+$ and $[M+2H]^{2+}$ types were seen at *m/z* = 562.791 and 595.906.

The FT-IR spectra of the ligands L^1 and L^2 showed the peaks of the ν(CH=N) azomethine group at 1604 and 1602 cm^{-1}. The participation of palladium ions in the form of ligands gave rise to the peaks of the azomethine group to shift to lower frequencies in both complexes at 1596 cm^{-1} [21,22].

In the FT-IR spectra of ligands L^1 and L^2, ligands exhibited broad bands at 3430, 3385, and 3426 cm^{-1} which were assignable to ν(OH), and bands at 1182 and 1173 cm^{-1} that can be attributed to the C–O

Table 1
TGA data of Schiff base-Pd(II) complexes.

Complexes	Step	TG range (°C)	Mass loss (%) Calc./Found		Assignment
[L^1Pd(H_2O)] H_2O•Cl 563.39 g/mol	1	50–800	54.74	53.75	$2H_2O$, Cl, $C_{14}H_{22}O_3$
	Residue	800-	45.26	46.22	C_7HN_2SPd
[L^2PdCl(H_2O)]H_2O 593.41 g/mol	1	50–430	67.65	67.93	$2H_2O$, Cl, $C_{19}H_{27}O_4N$
	2	440–800	6.06	5.64	C_3
	Residue	800-	26.29	26.43	C_3NOSPd

stretching vibrations. In the FT-IR spectra of complexes 1 and 2, the absence of the ν(OH) vibration confirmed the coordination of phenolic oxygen to the palladium ion. Furthermore, the phenolic ν(C–O) stretching vibration ligands shifted the lower wavenumber in complexes 1 and 2, showing that the phenolic oxygen is coordinated with the palladium ions [23]. The bands observed in the 1712 and 1710 cm^{-1} were commented as belonging to the (C=O) band in ligands L^1 and L^2. The peak due to ν(C=O) shifted to a higher frequency in complex 1. This showed that the oxygen atom of the (C=O) group coordinates with the palladium ion. In complex 2, the carbonyl band did not alter significantly.

The FT-IR spectra of complexes 1 and 2 observed bands at 3445 and 3542 cm^{-1} were assigned to the OH of the H_2O molecule [24]. These peaks were not seen at the ligands L^1 and L^2 spectrums. There were new signals that ranges from 554 to 590 cm^{-1} which were assigned to M-O and 459 to 502 cm^{-1} for M-N stretching frequencies [25]. The other main group did not show any notable change in their frequency. This showed that ligand L^1 was bonded to the palladium ion by the azomethine nitrogen, phenolic oxygen, carbonyl, and the oxygen atom of the coordination water. The ligand L^2 was bonded to the palladium ion by the azomethine nitrogen, phenolic oxygen, chlorine atom, and the oxygen atom of the coordination water.

The ^{1}HNMR spectra of complex 1 indicated the following characteristic chemical shifts: the singlet signal at 10.27 ppm showed the presence of the proton of the –NH, the singlet signal at 8.87 ppm showed the presence of the proton of CH=N of the azomethine group, the multiplet signal at 7.69 to 6.54 showed the presence of the protons of Ar. –CH, the multiplet signal at 4.31 showed the existence of the protons $–OCH_2$, the singlet signal at 2.51 ppm showed the existence of the proton of $–CH_2$ of pyridine, the singlet signal at 1.31 ppm showed the existence of the proton of $–OCH_2CH_3$ and the singlet signal at 1.46 to 1.13 ppm showed the existence of the protons of $–CH_3$ group. Similarly, the chemical shift values of complex 2 were given in the experimental section. The ^{1}HNMR spectra of complexes 1 and 2 indicated azomethine protons as singlets at 8.87 and 8.87 ppm. The downfield shift of peaks seen in the spectrum of L^1 and L^2 (8.82 and 8.80 ppm) verified the formation of complexes. The formation of complexes 1 and 2 was also verified by the disappearance of the OH signals.

In the ^{13}CNMR spectra of ligands L^1 and L^2, the carbons of the azomethine group were seen at 163.39 and 163.33 ppm. These signals downfield suggested that the azomethine nitrogen was coordinated with the metal ion in the ^{13}CNMR spectra of complexes 1 and 2. The signal of aromatic carbons in the ligands L^1 and L^2, 153.24–116.34 ppm, shifted to 155.95–117.06 ppm. That means; the phenolic oxygen was coordinated with the metal ion. The carbonyl carbon at 163.39 ppm in ligand L^1 shifted to downfield at 164.68 ppm in complex 1. The other data were given in the experimental part.

The UV–vis. spectra of complexes 1 and 2 were performed at room temperature and in 10^{-5} M ethanol solution at 200–800 nm. The UV–vis. spectra of complexes 1 and 2 showed max. absorption bands in the 217–261 nm which was corresponding to the π→π* transition of the aromatic chromophore groups and 305–395 nm which was attributed to the n→π* transition of azomethine [26]. The low energy peaks at 406–577 nm were because of mixed D-d transition of ligand to metal charge transfer transition and inter ligand charge transfer, with metal to ligand charge transfer transition [27,28]. The UV–Vis. spectra indicated that complexes 1 and 2 showed absorption bands at higher wavelengths and this showed that the complexes occurred.

The thermograms of complexes 1 and 2 were given in SM11 and SM12 in Supplementary Materials. The thermal decompositions of complexes 1 and 2 were performed up to 800 °C under a nitrogen atmosphere with a heating rate of 10 °C/min^{-1}.Table 1 summarized their thermal behaviors. The complex 1 decomposed thermally in a single step with a T_{DTG} peak 227.38 °C. The 54.74% mass loss occurring in the structure of complex 1 range of 50–800 °C corresponded to the degradation of the two water molecules, one chlorine atom, and $C_{14}H_{22}O_3$ organic moiety (calc. 54.74% found 53.75%) [29]. The final residue attributed to the C_7HN_2SPd moiety. The complex 2 decomposed thermally in two steps, the first of which occurred at 50–430 °C with a T_{DTG} peak 276.32 °C. This may be due to the loss of two H_2O molecules, Cl atom, and $C_{19}H_{27}O_4N$ moiety. The second and final dissociation step, the temperature range of 440–800 °C, associated with the elimination of the ligand moiety with a mass loss of 6.06 (5.64%) leaving a solid residue of C_3NOSPd.

3.2. Powders X-ray diffraction (XRD) study

The Schiff base-Pd(II) complexes (1, 2) were obtained only in powder form, which was not appropriate for a single X-ray diffraction analysis. To identify the degree of crystal structure in metal complexes, an X-ray powder diffraction pattern for complexes 1 and 2 was obtained. The

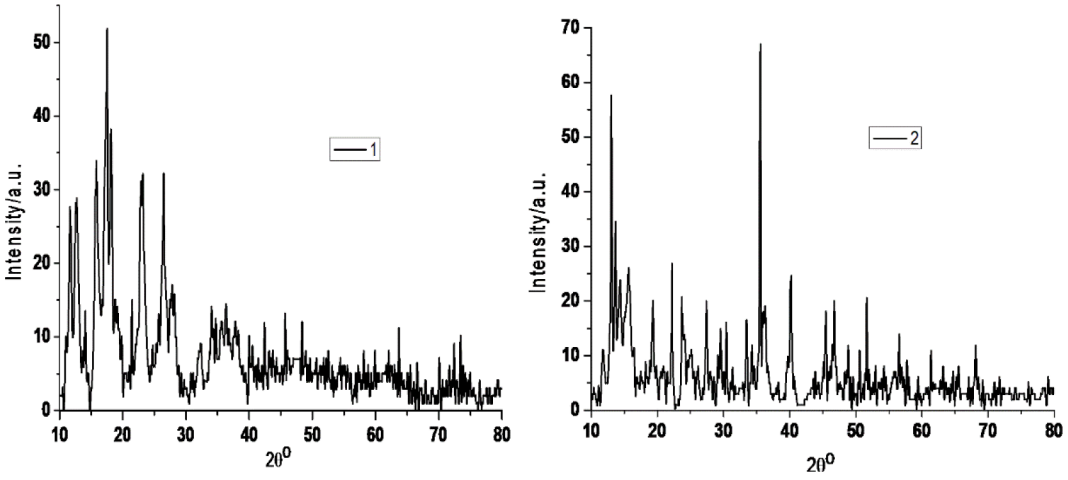

Fig. 2. Powder XRD spectra of complexes 1 and 2.

Table 2
Calculated powder XRD properties of complexes 1 and 2.

2 Theta (°)	FWHM (°)	Intensity	% Relative intensity	D nm	Average
11.641	0.434	27.82857	51.2	18.39967	1
12.74	0.521	29	51.8	15.34288	19.81888
15.859	0.493	34.08571	66,5	16.26974	
17.52	0.618	52.08571	100	13.00656	
18.121	0.279	38.42857	54.8	28.83393	
21.458	0.136	15.17143	27.5	59.45321	
23.141	0.7	32.34286	60.2	11.58439	
26.48	0.46	32,42,857	61.2	17.74178	
27.742	0.758	17.25714	22.8	10.79541	
34.077	0.332	12.65714	15.5	13.08976	
36.34	0.623	14.65714	19.4	25.02707	
37.8	0.572	12.25714	16.6	13.42089	
11.878	0.485	43.11553	11.2	16.46837	2
13.022	1.91E-01	57.82857	82.8	41.86315	27.93293
13.582	0.315	34.74286	25.3	25.39816	
14.455	0.417	24	14.3	19.20364	
15.66	0.711	26.25714	31.1	11.27856	
19.283	0.474	20.25714	22.6	17.00023	
22.221	0.244	27	44.9	33.18045	
23.718	0.323	20.91429	28.8	25.13173	
27.422	0.357	20.17143	30.8	22.90564	
30.421	0.141	16.25714	23.1	58.38789	
33.461	0.223	16.74286	24.8	37.19928	
35.542	0.291	67.17143	100	28.66788	
40.12	0.455	23.82857	37	18.58761	
45.48	0.268	18.34286	26.5	32.14126	
46.723	0.416	13.5128	27.2	20.80219	
51.659	0.228	9.96443	31.2	38.71079	

diffracted intensities of the complexes were measured utilizing the Ultima IV X-ray diffractometer (Rigaku with CuKα 0.1,540,562 nm). These are some manifestations of XRD operating the circumstances: Continuous scanning with a scan step of 0.02°, a scanning range of 10 to 80°, a scanning mode of 2Theta/Theta, an operating current of 40 mA, and an operating voltage of 40 kV. Fig. 2 revealed the XRD diffraction patterns of them. Through the use of Scherer's equation, we computed the complexes' grain sizes;

$$D = \frac{z\lambda}{F.Cos\theta} \quad (1)$$

X-ray wavelength, Bragg's diffraction angle, spherical crystals with cubic symmetry, and full width of half maximum intensity are shown by the symbols, λ, θ, z.1.54, and F respectively. From the maximum peak intensity, the complex's average grain sizes (D) were tabulated. Table 2 displays the crystal properties of these complexes, with all peaks rising to 10% of the greatest peak's height (FWHM, grain size, observed diffraction angle, intensity, and% relative intensity).

The XRD phase behavior of complex 1 is shown in Fig. 2. Several high-intensity peaks were observed by XRD. The highest intensity at the peak was 17.52°, while the lowest was 27.74° When these XRD powder peaks were matched to the MDI JADE library, they were found to be similar to the monoclinic crystal structure of ferulic acid $C_{10}H_{10}O_4$ (PDF#41–1606). Complex 1 has an average grain size of 19.82 nm and all its values are listed in Table 2. Our results showed that the largest grain was obtained at a diffraction angle of 21.46° (59.45 nm); the lowest was obtained at a diffraction angle of 27.74° (10.80 nm).

The XRD phase behavior of complex 2 is shown in Fig. 2. Some peaks with higher intensity than XRD were observed. The highest intensity was at peak 35.54°, while the lowest was at peak 11.88° When these XRD

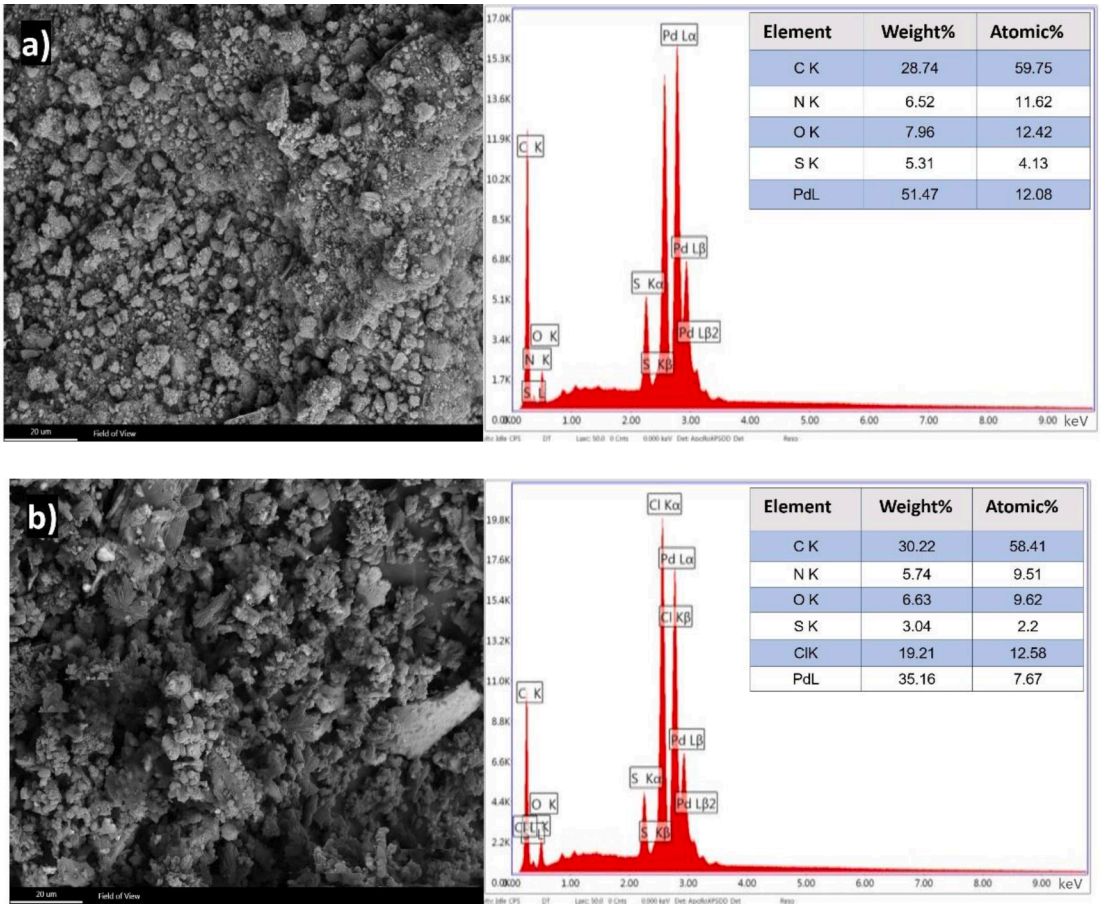

Fig. 3. SEM-EDX analysis of complexes 1 and 2.

powder peaks were fitted to the MDI JADE library, they were found to resemble the monoclinic crystal structure of 5-(1-methylethyl)−5-(2-propenyl)−2,4,6(1H,3H,5H)-pyrimidinetrione $C_{10}H_{14}N_2O_3$ (PDF#51–2373). Complex 2 has an average grain size of 27.93 nm and all its values are shown in Table 2. Our results showed that the largest grain was obtained at a diffraction angle of 30.42° (58.39 nm); the lowest was obtained at a diffraction angle of 15.66° (11.28 nm).

3.3. SEM-EDX analysis

Element symbols, weights, and atomic percentages of each element belonging to $[L^1Pd(H_2O)]Cl{\cdot}H_2O$ and $[L^2PdCl(H_2O)]H_2O$ complexes are shown in the SEM-EDX spectrum in Fig. 3a and b, respectively. C, N, O, S, and Pd peaks were obtained in the spectrum of the $[L^1Pd(H_2O)]Cl{\cdot}H_2O$ complex in Fig. 3a, their atomic percentage ratios were recorded as 59.75, 11.62, 12.42, 4.13, and 12.08, respectively. In the spectrum of the $[L^2PdCl(H_2O)]H_2O$ complex in Fig. 3b, C, N, O, S, Cl, and Pd peaks were obtained, with atomic percentage ratios were recorded as 58.41, 9.51, 9.62, 2.20, 12.58, and 7.67, respectively. The element percentages obtained in CHNS analyses were close to the amounts obtained in the EDX spectrum. In addition, the presence of Pd and Cl in both complexes was confirmed.

3.4. Suzuki-Miyaura and Mizoroki-Heck reactions

The Suzuki-Miyaura reaction is a highly effective method for the formation of C—C bonds by combining various organic moieties with different reagents such as aryl, vinyl, and alkyl halide organoborane reagents.

The Suzuki-Miyaura cross-coupling reaction was carried out in a Schlenk flask. Schiff base-Pd(II) complex (0.01 mmol), aryl bromide (2.0 mmol), phenylboronic acid (3.0 mmol), K_2CO_3 (4.0 mmol), EtOH/H_2O (5 mL) were added to a small Schlenk tube in open air atmosphere. The reaction mixture was heated 80 °C for 2 h. The base, solvent, temperature, and catalyst loading were examined and optimized (Table 3). Samples were taken at regular intervals and the completion of the reaction was checked by GC. After concluding that the reaction was over, the mixture was cooled. Then the organic phase was taken with ethyl acetate/hexane (1:5). The resulting mixture was completely purified from water and moisture with $MgSO_4$ and passed through a silica gel column to be given to GC–MS. The best conversion was obtained with the best choice for the base (K_2CO_3) in 2 h with 95% efficiency.

Table 4
Solvent optimization reaction conditions for the Suzuki-Miyaura reaction.

Entry	Solvent	Time (h)	Yield (%)
1	Ethanol	3	72
2	Methanol	3	60
3	Acetonitrile	3	35
4	Toluene	3	52
5	DMF	3	41
6	THF	3	39
7	Dioxane	3	41
8	*i*-PrOH+H_2O	3	76
9	Ethanol+H_2O	2	95
10	Ethanol+H_2O	1	62

Reaction conditions: Phenylboronic acid (3.0 mmol), aryl bromide (2.0 mmol), K_2CO_3 (4.0 mmol), catalyst (0.01 mmol), EtOH/H_2O (5 mL 1:2), and 80 °C.

When Table 4 was evaluated, the solvent selection was made by trying organic and inorganic solvents. It was found that the best solvent choice was the ethanol-water mixture.

Pd(II) complexes were used to determine their performance under optimal conditions, and to study the reaction between aryl bromide and phenylboronic acid. After the optimization conditions were determined, the effect of the aryl bromide containing aryl halide in Table 5 was investigated using both Pd(II) complexes 1 and 2. Excellent conversion (88–99%) was observed with aryl bromides derivatives (4-bromobenzaldehyde, 4-bromobenzene, and 4-bromoacetophenone, etc.) containing no substituents on the aromatic ring and especially having carbonyl groups. Excellent and high (67–91%) conversions were obtained with 4-bromoanisole and 4-bromotoluene (entries 1–4, 5–8, 9–10). In general, high conversions and excellent yields were achieved for both catalysts (1 and 2). However, using 4-bromotoluene as an electronically deactivated substrate for the Suzuki-Miyaura cross-coupling reaction gave relatively good yields (67% and 71%) (entries 7 and 8).

The catalysts were found to be highly effective, with good to excellent catalytic activity and product selectivity against unsaturated and different functional groups of aryl bromides under the same conditions (entries 1–5 and 9–10). For example, very high isolated yields (>90%) and complete conversions were obtained when 4-bromobenzaldehyde was coupled with phenylboronic acid with our catalyst system (entries 3, 4). The best yield was obtained using 4-bromobenzene as the aryl bromide. Based on the results obtained, when the catalytic activities are evaluated between the two complexes, it is thought that there is no

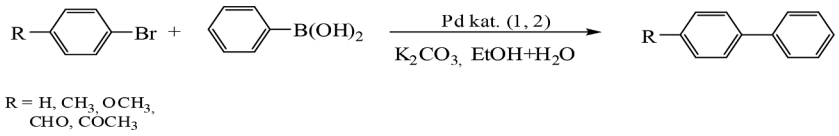

Table 3
Base optimization reaction conditions for the Suzuki-Miyaura reaction.

Entry	Base	Time (h)	Yield (%)
1	NaOH	3	51
2	Cs_2CO_3	3	46
3	KOH	3	58
4	K_2CO_3	3	95
5	$KOBu^t$	3	40
6	–	3	–
7	K_2CO_3	2	95*
8	K_2CO_3	2	95
9	K_2CO_3	1	62

Reaction conditions: Phenylboronic acid (3.0 mmol), aryl bromide (2.0 mmol), K_2CO_3 (4.0 mmol), Catalysis amount (Pd(II) comp. (0.01 mmol), EtOH/H_2O (5 mL 1:2), and 80 °C. *Catalysis amount (Pd(II) comp. (0.02 mmol)).

Table 5
Suzuki-Miyaura coupling reactions catalyzed by Pd(II) complexes.

Entry	Pd(II) complexes	Aryl halides	Time (h)	Temperature (°C)	Yield (%)
1	1		2	80	88
2	2				96
3	1		2	80	91
4	2				95
5	1		2	80	91
6	2				70
7	1		2	80	67
8	2				71
9	1		2	80	98
10	2				99

Reaction conditions: Phenylboronic acid (3.0 mmol), aryl halide (2.0 mmol), base (4.0 mmol), catalyst (0.01 mmol), EtOH/H_2O (5 mL), 2 h and 80 °C.

significant difference between them and that they are active thanks to the active groups in the ligand in both complexes [16,30].

The catalytic activity of the existing complexes is good, and although a similar catalytic system has been reported in the literature, this type of catalyst is new for the bidentate O, N-donor medium containing palladium center and different donor atom (O, N, and S). It is very important to note that in all cases of this study, the reactions were carried out both in the air and using only less than 0.01 mmol of catalyst. In similar literature studies, both inert media and high-rate catalysts were used.

The scope of the Heck reaction was carried out between various substituted aryl bromides and styrene, with optimized reaction conditions by experimenting with different conditions. Reactions with aryl bromides took place in Et-OH/H_2O (1:2) mixture for 2 h.

Between aryl bromides containing an electron-donating methoxy group (Table 6, entries 5, 6) or an electron-withdrawing group (Table 6, entries 3, 4) and styrene, the desired products were obtained with 79–87% yields of both catalysts under optimized conditions. The reaction of aryl bromide substrates with styrene under optimized conditions resulted in yields of 69–75% of the desired coupling products. The results of using aromatic bromide and various substituents as functional groups are shown in Table 6. Thus, the use of *p*-bromo containing aromatic halides confirms the performance of the Pd(II) complexes 1 and 2 in the Mizoroki-Heck coupling reaction. As a result, the use of electro-withdrawing and electron-releasing groups in the aromatic ring and the use of substrates such as bromobenzene that do not contain any substituents show that the catalysts are active in terms of structural activity [30].

Under optimized conditions, low catalyst loading tests were performed for complexes 1 and 2 with aryl bromide and styrene. The catalyst completed the reaction in 2 h in 87% yield using 0.01 mol% catalyst (Table 6, entry 3). Further lowering of the catalyst loading was seen to greatly reduce the yield within 2 h (entry 3). However, with a longer reaction time of up to 12 h, the yield of 87% was not exceeded (entry 4). It has been reported that it is difficult to obtain complete conversion for the reaction of bromoanisole with styrene in Heck catalysis, but complex 1 showed excellent activity in Heck coupling with 86% yield [17,31]. By running the reaction for 2 h using 0.01 mol% catalyst, catalysts 1 and 2 yielded 69–86% efficiency. In addition, the observed catalytic activities of both of our catalysts are thought to be due to the functional groups in the ligand's structure.

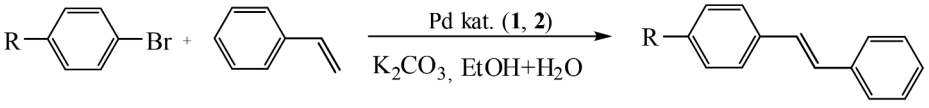

R= H, CH_3, OCH_3, CHO, $COCH_3$

Table 6
Mizoroki-Heck coupling reactions catalyzed by Pd(II) complexes.

Entry	Pd(II)	Aryl halides	Time (h)	Temperature (°C)	Yield (%)
1	1		2	80	69
2	2				75
3	1		2	80	87
4	2				81
5	1		2	80	86
6	2				79
7	1		2	80	74
8	2				70
9	1		2	80	70
10	2				73

Reaction conditions: Styrene (3.0 mmol), aryl bromide (2.0 mmol), K_2CO_3 (4.0 mmol), catalyst (0.01 mmol), EtOH/H_2O (5 mL, 1:2), 2 h and 80 °C.

4. Conclusion

The Schiff base-Pd(II) complexes were synthesized and characterized using physicochemical and spectroscopic techniques. The molecular structures of complexes were suggested according to the results gained from the analytical and spectroscopic techniques. The results showed that the Schiff base-Pd(II) complexes had square planar geometry when coordinated with the tridentate ONO form L^1 and the bidentate NO donor ligand form L^2. These complexes displayed excellent catalytic activities in Suzuki-Miyaura and Mizoroki-Heck cross-coupling reactions. The results gained from Suzuki-Miyaura and Mizoroki-Heck reactions show that electron-withdrawing and electron-donating substituents on aryl halide can produce the coupling products in perfect yield in the existence Pd(II) complexes. This study will shed light on the study to be done in this field.

Credit author statement

The manuscript was designed by Nevin Turan and Abbas Akdeniz. Nevin Turan and Abbas Akdeniz performed the synthesis, characterization and catalytic studies. Nevin Turan coordinated the manuscript writing. Nevin Turan supervised the overall work. The authors have approved the final version of the manuscript.

Declaration of Competing Interest

No conflict of interest was declared by the author.

Data availability

Data will be made available on request.

Acknowledgment

This work was financially supported by the unit of Scientific Research Projects, Muş Alparslan University, Muş/Turkey (Project no: BAP-20-FEF-4902–06).

Supplementary materials

Supplementary material associated with this article can be found, in the online version, at doi:10.1016/j.molstruc.2023.135724.

References

[1] M.N. Uddin, S.S. Ahmed, S.M.R. Alam, Review: biomedical applications of Schiff base metal complexes, J. Coord. Chem. 73 (23) (2020) 3109–3149, https://doi.org/10.1080/00958972.2020.1854745.
[2] M. Bingöl, N. Turan, Schiff base and metal(II) complexes containing thiophene-3-carboxylate: synthesis, characterization and antioxidant activities, J. Mol. Struct. 1205 (2020), 127542, https://doi.org/10.1016/j.molstruc.2019.127542.
[3] S.I. Al-Saeedi, L.H. Abdel-Rahman, A.M. Abu-Dief, S.M. Abdel-Fatah, T.M. Alotaibi, A.M. Alsalme, A. Nafady, Catalytic oxidation of benzyl alcohol using nanosized Cu/Ni Schiff-base complexes and their metal oxide nanoparticles, Catalysts 8 (10) (2018) 452, https://doi.org/10.3390/catal8100452.
[4] M.S. More, P.G. Joshi, Y.K. Mishra, P.K. Khanna, Metal complexes driven from Schiff bases and semicarbazones for biomedical and allied applications: a review, Mater. Today Chem. 14 (2019), 100195, https://doi.org/10.1016/j.mtchem.2019.100195.
[5] P. Surendar, T. Pooventhiran, S. Rajam, A. Irfan, R. Thomas, Schiff bases from α-ionone with adenine, cytosine, and L-leucine biomolecules: synthesis, structural features, electronic structure, and medicinal activities, J. Comput. Biophys. Chem. 21 (2022) 1–22, https://doi.org/10.1142/S2737416522500016.
[6] T. Akram, M. Athar, A. Mahmood, E. Barboza, D. Lima, F. Perveen, M. Ashraf, I. Ahmad, S. Goumri-said, Synthesis, molecular structure, spectroscopic properties and biological evaluation of 4-substituted-N-(1H-tetrazol-5-yl) benzenesulfonamides: combined experimental, DFT and docking study, J. Mol. Struct. 1195 (2019) 119–130, https://doi.org/10.1016/j.molstruc.2019.05.065.
[7] Y. Al-Khafaji, N. Abd Alrazzak, T. Saad, S. Abbas, M. Merdan, Aluminium complexes as catalysts for ring-opening polymerization of ε-caprolactone bearing Schiff base ligands derived from 4,4′-methylenebis (2,6-diisopropylaniline), J. Phys. Conf. Ser. 1234 (2019), 012055, https://doi.org/10.1088/1742-6596/1234/1/012055.
[8] X. Liu, C. Manzur, N. Novoa, S. Celedón, D. Carrillo, J.R. Hamon, Multidentate unsymmetrically substituted Schiff bases and their metal complexes: synthesis, functional materials properties, and applications to catalysis, Coord. Chem. Rev. 357 (2018) 144–172, https://doi.org/10.1016/j.ccr.2017.11.030.
[9] S. Chakrabortty, M. Kaur, M. Adhikari, K.K. Manar, S. Singh, A bis (BICAAC) palladium(II) complex: synthesis and implementation as catalyst in Heck-Mizoroki and Suzuki-Miyaura cross coupling reactions, Inorg. Chem. 60 (9) (2021) 6209–6217, https://doi.org/10.1021/acs.inorgchem.0c03614.
[10] L. Sun, Q. Li, M. Zheng, S. Lin, C. Guo, L. Luo, S. Guo, Y. Li, C. Wang, B. Jiang, Efficient Suzuki-Miyaura cross-coupling reaction by loading trace Pd nanoparticles onto copper-complex-derived Cu/C-700 solid support, Colloid Interface. Sci. 608 (2022) 2463–2471, https://doi.org/10.1016/j.jcis.2021.10.174.
[11] W. Al Zoubi, A.A.S. Al-Hamdani, S.D. Ahmed, Y.G. Ko, Synthesis, characterization, and biological activity of Schiff bases metal complexes, J. Phys. Org. Chem. 31 (2) (2018) e3752, https://doi.org/10.1002/poc.3752.
[12] A. Rajmane, S. Jadhav, A. Kumbhar, N, O-polydentate ligands for palladium-catalyzed cross-coupling reactions (Part III), J. Organomet. Chem. 957 (2022), 122147, https://doi.org/10.1016/j.jorganchem.2021.122147.
[13] S. Urus, M. Keles, O. Serindag, Catalytic synthesis of 2-methyl-1,4-naphthoquinone (vitamin K3) over silica-supported aminomethyl phosphine-Ru(II), Pd(II), and Co (II) complexes, Phosphorus Sulfur Silicon Relat. Elem. 185 (7) (2010) 1416–1424, https://doi.org/10.1080/10426500903061533.
[14] J.C. Hierso, A. Fihri, R. Amardeil, P. Meunier, H. Doucet, M. Santelli, Use of a bulky phosphine of weak α-donicity with palladium as a versatile and highly-active catalytic system: allylation and arylation coupling reactions at 10^{-1}-10^{-4} mol% catalyst loadings of ferrocenyl bis(difurylphosphine)/Pd, Tetrahedron 61 (41) (2005) 9759–9766, https://doi.org/10.1016/j.tet.2005.06.065.
[15] A. Kilic, E. Gezer, F. Durap, M. Aydemir, A. Baysal, Pd(II) supported dioxime functionalized Fe_3O_4 nanoparticles as efficient, eco-friendly and reusable catalysts for the Suzuki-Miyaura cross-coupling reaction in water, J. Organomet. Chem. 896 (2019) 129–138, https://doi.org/10.1016/j.jorganchem.2019.06.007.
[16] E. Tas, A. Kilic, M. Durgun, I. Yilmaz, I. Ozdemir, N. Gurbuz, Mono- and dinuclear Pd(II) complexes of different salicylaldimine ligands as catalysts of transfer hydrogenation of nitrobenzene with cyclohexene and Suzuki-Miyaura coupling reactions, J. Organomet. Chem. 694 (3) (2009) 446–454, https://doi.org/10.1016/j.jorganchem.2008.11.021.
[17] A. Kilic, D. Kilinc, E. Tas, I. Yilmaz, M. Durgun, I. Ozdemir, S. Yasar, The orthopalladation dinuclear $[Pd(L_1)(\mu\text{-}OAc)]_2$, $[Pd(L_2)(\mu\text{-}OAc)]_2$ and mononuclear $[Pd(L_3)_2]$ complexes with [N, C, O] or [N, O] containing ligands: synthesis, spectral characterization, electrochemistry and catalytic properties, J. Organomet. Chem. 695 (5) (2010) 697–706, https://doi.org/10.1016/j.jorganchem.2009.12.003.
[18] S. Iyer, G.M. Kulkarni, C. Ramesh, Mizoroki-Heck reaction, catalysis by nitrogen ligand Pd complexes and activation of aryl bromides, Tetrahedron 60 (9) (2004) 2163–2172, https://doi.org/10.1016/j.tet.2003.12.012.
[19] N. Turan, K. Buldurun, N. Çolak, İ. Özdemir, Preparation and spectroscopic studies of Fe(II), Ru(II), Pd(II) and Zn(II) complexes of Schiff base containing terephthalaldehyde and their transfer hydrogenation and Suzuki-Miyaura coupling reaction, Open Chem. 17 (1) (2019) 571–580, https://doi.org/10.1515/chem-2019-0074.
[20] A. Akdeniz, Investigation of synthesis, characterization and catalytic activities of Schiff base ligands and transition metal complexes. Master Thesis, Natural and Applied Science, Muş Alparslan University, Muş/Turkey, (2022).
[21] A. Jamshidvand, M. Sahihi, V. Mirkhani, M. Moghadam, I. Mohammadpoor-Baltork, S. Tangestaninejad, H. Amiri Rudbari, H. Kargar, R. Keshavarzi S. Gharaghani, Studies on DNA binding properties of new Schiff base ligands using spectroscopic, electrochemical and computational methods: influence of substitutions on DNA-binding, J. Mol. Liq. 253 (2018) 61–71, https://doi.org/10.1016/j.molliq.2018.01.029.
[22] Y. Li, Z. Yang, DNA-binding properties and antioxidant activity of lanthanide complexes with the Schiff base derived from 3-carbaldehyde chromone and isonicotinyl hydrazine, J. Coord. Chem. 63 (2010) 1960–1968, https://doi.org/10.1080/00958972.2010.496127.
[23] A.M. Tajuddin, H. Bahron, K. Kassim, W.N.W. Ibrahim, B.M. Yamin, Synthesis and characterization of palladium(II) Schiff base complexes and their catalytic activities for Suzuki coupling reaction, Malaysian J. Anal. Sci. 16 (1) (2012) 79–87.
[24] N. Turan, K. Buldurun, E. Bursal, G. Mahmoudi, Pd(II)-Schiff base complexes: synthesis, characterization, Suzuki-Miyaura and Mizoroki-Heck cross-coupling reactions, enzyme inhibition and antioxidant activities, J. Organomet. Chem. 970-971 (2022), 122370, https://doi.org/10.1016/j.jorganchem.2022.122370.
[25] M.E. Alkış, K. Buldurun, N. Turan, Y. Alan, Ü. Keleştemur Yılmaz, A. Mantarcı, Synthesis, characterization, antiproliferative of pyrimidine based ligand and its Ni (II) and Pd(II) complexes and effectiveness of electroporation, J. Biomol. Struct. Dyn. 40 (9) (2020) 4073–4083, https://doi.org/10.1080/07391102.2020.1852965.
[26] E.S. Aazam, A.F. EL-Husseiny, H.M. Al-Amri, Synthesis and photoluminescent properties of a Schiff-base ligand and its mononuclear Zn(II), Cd(II), Cu(II), Ni(II) and Pd(II) metal complexes, Arabian J. Chem. 5 (1) (2012) 45–53, https://doi.org/10.1016/j.arabjc.2010.07.022.
[27] A. Zianna, G.D. Geromichalos, A. Pekou, A.G. Hatzidimitriou, E. Coutouli-Argyropoulou, M. Lalia-Kantouri, A.A. Pantazaki, G. Psomas, A palladium(II) complex with the Schiff base 4-chloro-2-(N-ethyliminomethyl)-phenol: synthesis, structural characterization, and *in vitro* and in silico biological activity studies, J. Inorg. Biochem. 199 (2019), 110792, https://doi.org/10.1016/j.jinorgbio.2019.110792.

[28] H. Kargar, V. Torabi, A. Akbari, R.B. Ardakani, A. Sahraei, M.N. Tahir, Pd(II) and Ni(II) complexes containing an asymmetric Schiff base ligand: synthesis, X-ray crystal structure, spectroscopic investigations and computational studies, J. Mol. Struct. 1205 (2020), 127642, https://doi.org/10.1016/j.molstruc.2019.127642.

[29] N. Turan, Synthesis, spectroscopic characterization, optical characteristics and parameters of two new cobalt, palladium complexes and Schiff base ligand, J. Electron. Mater. 48 (11) (2019) 7366–7371, https://doi.org/10.1007/s11664-019-07562-3.

[30] K. Buldurun, T. Sarıdağ, Synthesis of Pd^{+2} complexes of Schiff bases containing methyl 2-amino-6-benzyl-4,5,6,7-tetrahydrothieno[2,3-*c*]pyridine-3-carboxylate and spectral and catalytic activities, J. Mol. Struct. 1273 (2023), 134278, https://doi.org/10.1016/j.molstruc.2022.134278.

[31] W.H. Yang, C.S. Lee, S. Pal, Y.N. Chen, W.S. Hwang, Ivan J.B. Lin, J.C. Wang, Novel Ag(I), Pd(II), Ni(II) complexes of N,N′-bis-(2,2-diethoxyethyl)imidazole-2-ylidene: synthesis, structures, and their catalytic activity towards Heck reaction, J. Organomet. Chem. 693 (25) (2008) 3729–3740, https://doi.org/10.1016/j.jorganchem.2008.09.017.